Landfill interface study on liner member selection, stability assessment, and factor of safety predictions with seismic loading

M. Saravanan[1], M. Kamon[2], H.A. Faisal[2], T. Katsumi[4], T. Akai[5], T. Inui[6], and A. Matsumoto[5]

[1)] Graduate Student, Graduate School of Global Environmental Studies, Kyoto University, Japan
[2)] Professor, Graduate School of Global Environmental Studies, Kyoto University, Japan
[3)] Professor, Department of Civil Engineering, Faculty of Engineering, University Malaya, Malaysia
[4)] Associate Professor, Graduate School of Global Environmental Studies, Kyoto University, Japan
[5)] Senior Research Scientist, Technology Research Institute of Osaka Prefecture, Osaka, Japan
[6)] Assistant Professor, Graduate School of Global Environmental Studies, Kyoto University, Japan

ABSTRACT : Recent landfill failures have indicated that failures are occurring along the low interface friction angle zone within landfill liner components. This has lead to the researches to be carried on the internal and interface shear strength properties of landfill liner components, which consist of subsoils, compacted clay liners (CCLs) , geosynthetic clay liners (GCLs), geomembrances and geotextiles. The soil-geomembrane or any other liner interface combination could act as a possible plane of potential instability of the liner under static and seismic loading (Hoe et al. 1997). Hence, this paper addresses part of our continuing research to investigate the important factors, which should be considered by geotechnical engineers designing landfills, to prevent failures due to poor interface properties under static and earthquake induce forces (seismic loading) for both based and cover soil liners. Interface stress and horizontal strain behaviour for various liner configuration was studied to understand the peak and residual shear stress trend to select suitable liner configuration which can act as a composite member during failure. Understanding the stress and horizontal strain behaviour of liner member component is critical in order to allow the transfer of failure stress between interfacing member to resist continuous or progressive failure from occurring. Along with suitable liner selection approach, the conventional stability design on liner interface were also investigated using limit equilibrium method to study the influence of landfill geometry, normal loads (fill height), side and cover slope angles and seismic loading. The findings of the study are compiled into a simplified computation model to assist engineers in predicting and estimating the factor of safety (FOS) of the liner interface stability during design stages or for on-going filling work where the landfill geometry is continuously changing.

1. INTRODUCTION

Selecting the appropriate landfill liner depends mainly on the environmental protection regulations of an individual country, which often focus on protecting against leachate leakage. However, from geotechnical aspect, the landfill liner selection depends on the slope sections fill heights, interface properties, and horizontal strain compatibilities. Tables 1a, 1b and 2 present various combinations of laboratory interface test results and interface stress and horizontal strain behaviour of the tests obtained from Saravanan et al., 2006c, respectively. Stark et al. 1994, have presented design approach that uses a combination of the peak and residual shear strengths. However, the use of peak and residual shear strengths has uncertainty in the failure relationship between laboratory shear displacement, field shear displacement, the effect of progressive failure, and possible shear displacement due to an earthquake along the interface failure plane. Hence, various failure conditions required to be considered in interface design (Shark et al. 2004). The residual shear strength can be mobilized for many reasons, including waste settlement or creep that leads to shear displacement along specific interfaces (Long et al. 1995), waste placement activities (Yazdani et al. 1995), lateral movement or bulging of waste (Stark el al. 2000), construction activity of the liner system (McKelvey et al. 1994), thermal expansion/contraction of the geosynthetic material, stress transfer between the waste on the side slope and the landfill base that acts as a buttress (Stark et al. 1994), horizontal strain or displacement incompatibility between the waste and geosynthetic interface of interest (Eid et al. 2000), and earthquake induce displacements (Shark et al. 2004). These shear displacements may lead to the mobilization of residual strength, which can result in progressive failure effects between the side slope and at least a portion of the base of a bottom liner system (Stark et al. 1994, Gilbert et al. 1996, Reddy et al. 1996, Filz et al. 2001).

A failure envelope that corresponds to the lowest peak interface strength may also correspond to the strength of one or more interfaces because geosynthetic interface strength

is stress dependent and non-linear (Stark et al. 1994, Stark et al. 1996, Fox et al. 1998, Dove et al. 1999). If more than one interface parameter is used to develop the failure envelope of a liner with the lowest peak and residual strength, then the failure envelope is referred to as a composite failure envelope. In summary, designers should reconsider the use of minimum peak and residual failure envelope for design by determining which material will reach the peak and residual shear stress condition earlier with horizontal strain and use the corresponding parameters for peak and residual composite failure envelope for design. This can be achieved by establishing the stress and horizontal strain behaviour of every individual interface component with normal stresses and then evaluate the composite failure envelope trend.

2.0 LINER INTERFACE STRESS AND HORIZONTAL STRAIN BEHAVIOUR

Lower interface shear strengths between geomembranes and other geosynthetics can trigger a rapid failure during seismic loading conditions. Many researchers have discussed the interface shear strengths of landfill materials (e.g., Stark et al. 1994, Gilbert et al. 1996, Stark et al. 1996, Daniel et al. 1998, Palmeira et al. 2002, Chiu et al. 2004, Fox et al. 2004, Gourc et al. 2004, Kotake et al. 2004). The soil geomembrane interface acts as a potential plane of instability under both static and seismic loadings (Ling et al. 1997). Such interfaces have failed in the past due to low friction angle between the soil and the geosynthetic layers within the liner system. Therefore, the interface shear strength of any combination of liner materials requires meticulous study for safe design of new landfills. Hence, this paper examines some common landfill liner configurations in order to understand the possible modes of single and composite interface failure trend. A model liner configuration was studied, namely single member liner configuration (SMLC). The data and plots analyzed and presented in subsequent sections were obtained from Saravanan, Kamon et al. 2006a, 2006b, and 2006c.

2.1 Single Membrane Liner Configuration (SMLC)

Figure 1 shows the configuration of a single membrane liner with a geomembrane placed directly on native soil and protected from waste using a layer of geotextile. Table 3 lists the interface combinations and test results, while Figure 2 shows the plot of interface shear stress against normal stress. In addition, Figure 3 shows the stress and horizontal strain behaviour of the liner configuration listed in Table 3. Based on the stress and horizontal strain assessment, liner configuration SMLC A has failure horizontal strains within 1 to 3% with homogenous failure path as shown in Figure 4a. However, failure peak stresses are double for the interface in Test 27A, which is between smooth HDPE (Type 1) geomembrane and native soil, compared to the Test 1A interface, which is between geotextile and smooth HDPE (Type 1) geomembrane. These stress differences could cause a well-defined potential interface failure within geotextile and smooth HDPE (Type 1) geomembrane. For SMLC B and SMLC C, the SMLC B combination has similar peak shear stresses between interface Test 2A and interface Test 28A compared to SMLC C. These similarities could assist the liner to act as a composite member during failure, especially under low normal stress of 100 kPa, as shown in Figure 4b. For high normal stress, the variation in residual shear stresses is a disadvantage for the liner configuration. However, the failure horizontal strain of interface Test 2A needs to be prolonged to match the horizontal strain hardening effect of interface Test 28A. Hence, improving the textured HDPE geomembrane properties is necessary to provide a horizontal strain hardening effect similar to smooth surface HDPE geomembrane. However, for a single liner component, it is best to use textured HDPE geomembrane than smooth surface HDPE geomembrane for low normal stresses. The configuration of a geomembrane placed directly on native soil requires careful consideration against microscopic puncture with sufficient sacrificial thickness.

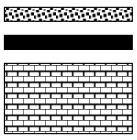

Figure 1 : Single membrane liner configuration (SMLC)

3 LIMIT EQUILIBRIUM ANALYSIS APPROACH

Further, to assess landfill liner stress and horizontal strain behaviour, conventional limit equilibrium design approach was studied for stability. Figure 5 shows a typical analysis model adopted for the study. The landfill base

and cover liner configurations are shown in Figures 6a and 6b, respectively. The model consist of 25m high landfill with 3H:1V cover slope angle and side slope angle of 3H:1V. Table 4 lists the interface test results and soil parameters for the liner configuration. Figures 7 and 8 summarize the interface test results and combined stress and horizontal strain plot for the landfill liner, respectively. Figure 9 shows the interface stress and horizontal strain behaviour of the liner configuration. As for the stability analysis, compatible software was used to model the landfill slope with relevant input parameters obtained from laboratory test data. Limit equilibrium based software was used to analyze both the static and seismic loading conditions. Table 5 lists the cases considered for analysis. All cases were analyzed for the as-installed conditions at optimum moisture content.

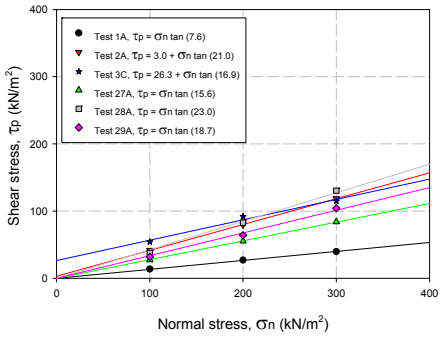

Figure 2 : Summary of the peak failure envelopes for a single membrane liner configuration (SMLC).

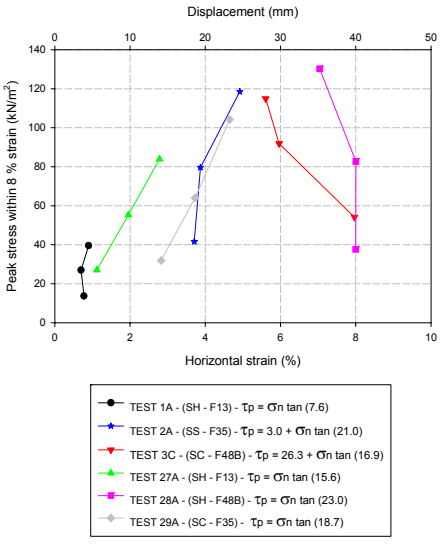

Figure 3 : Peak shear stress with horizontal strain for single membrane liner configuration (SMLC)

The stress and horizontal strain plot indicates that the interface between sand:bentonite mixture (100:10) and geotextile (Test 19A), and the interface between sand:bentonite mixture (100:10) and native soil (Test 23A) have horizontal strain hardening within a horizontal strain range between 4 ~ 8% and beyond (SH – F48B). This trend is vital to retain composite failure with a high residual strength during progressive failure. In the case of Test 2A, the interface between textured HDPE (Type 2) geomembrane and geotextile experiences horizontal strain softening with a failure horizontal strain between 4 ~ 6% (SS-F46). However, the failure trend in the residual region is higher for lower normal stresses (100 ~ 200 kPa) and is similar for high normal stresses when compared to the interface between sand:bentonite mixture (100:10) and geotextile (Test 19A). This behaviour could cause the interfaces between Test 2A and Test 19A to act as composite member during failure for high normal stresses. The composite behaviour could cause the failing interface plane to cut through other interface planes and indirectly gain resisting strength during progressive failure. Hence, understanding the stress and horizontal strain behaviour of a liner member component is critical in order to allow the transfer of failure stress between interfacing members and to resist continuous or progressive failure.

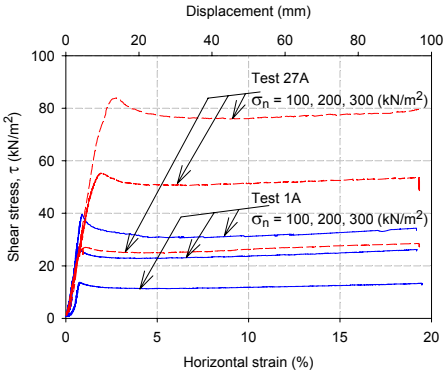

Figure 4a : Stress and horizontal strain behaviour for liner configuration SMLC A

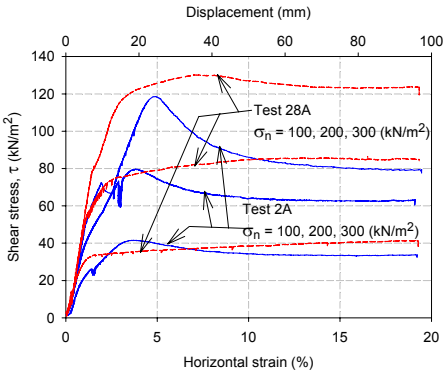

Figure 4b : Stress and horizontal strain behaviour for liner configuration SMLC B

Figures 10a, 10b, 10c, 10d and 10e shows typical analysis results for the cases listed in

Table 5. Seismic horizontal coefficients of 0.5, 0.1, 0.15, 0.2 and 0.25 were introduced in the analysis in order to study the trend of liner interface performance under earthquake-induced loading. Based on the interface stability analysis presented in Figure 11a, critical cases identified were 3, 6, 7 and 8, which demonstrate that the interface between the sand:bentonite mixture (100:10) and geotextile (Case 3) is the weakest with FOS reduced below unity with seismic loading exceeding coefficient of 0.15. Cases 6, 7 and 8 represent the interface stability for the cover liner section. In cover liner section, the lowest interface the Case 6 is between the geotextile and cover soil (highly weathered granitic soil - native soil) with FOS of 1.0 under static condition. This low interface indicates a high possibility of facial failure of the landfill cover. Deeper facial failure beyond the cover soil is resisted by HDPE (Type 2) geomembrane , in which the FOS drops below unity with seismic loading exceeding coefficient of 0.15.

These results are consistent with interface Test 19A, which has the lowest coefficient of friction as shown in Figures 7 and 8. However, in the case of landfill cover, the interface between geotextile and cover soil (Case 6) has high potential to failure during heavy rainfall under static condition and under seismic loading due to the poor interface property. The low FOS can be improved by providing benches on the cover slope. In the cases of 7 and 8, the interface of textured HDPE (Type 2) geomembrane with geotextile on the cover soil section has sufficient FOS until seismic loading coefficient of 0.15 is reached, as shown in Figure 11a. Although Case 6 and Case 3 have similar conditions, the base liner in Case 3 is more stable than the liner cover in Case 6. As shown in Figure 11b, the internal stability (Cases 2 and 9) and the overall stability (Case 12) of the landfill, the FOS obtained are relatively stable under both static and seismic loadings. Only in Cases of 10 and 11, as shown in Figure 11c, the toe and overall waste mass failure indicate a failure under minor seismic loading similar to Case 6. In this model, the most critical failure zone is at the cover soil area and waste mass failure closer to landfill cover. Hence, careful design of the cover slope section is critical. To summarize the stability analysis, the interface between sand:bentonite mixture (100:10) and geotextile (Case 3) is critical for base liner and Case 6 for liner cover under seismic conditions. However, the interface between geotextile and cover soil (Case 6) is also critical under static condition with FOS of only 1.0. Although Cases 3 and 6 have similar conditions, the base liner in Case 3 is more stable than the liner cover condition in Case 6, indicating that the influence of normal loads (fill height) is essential during seismic loading. Hence, alternative or improved linear materials should be investigated along with the liner design approach in order to design appropriate interface material combinations suitable for low normal loads such as shallow fill height for cover liner. To study further the influences of normal loads, landfill sections, side and cover slope angles, active and passive forces on the stability, and to provide a quick and compressive reference guide for engineers, four model cases were adopted for detail analysis on liner interface performance on landfill stability are discussed in the following section of simplified interface stability.

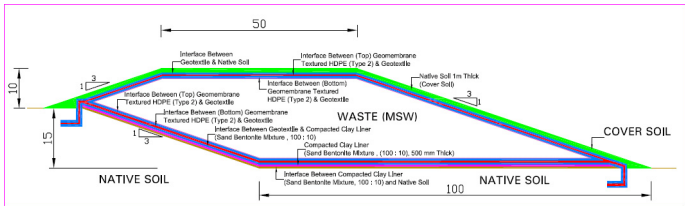

Figure 5 : Typical section of a landfill used in stability analysis.

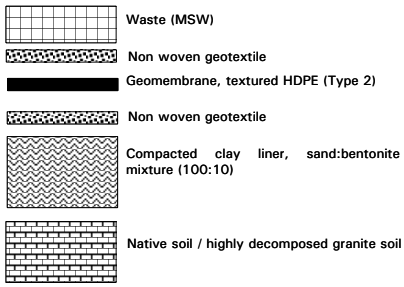

Figure 6a : Configuration of single composite landfill liner.

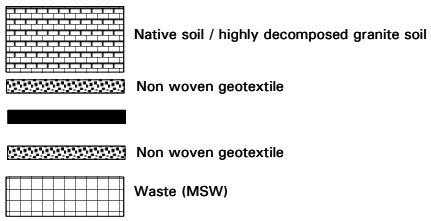

Figure 6b : Configuration of single membrane cover liner.

4 SIMPLIFIED INTERFACE STABILITY APPROACH

Numerous researchers have studied the interface properties and stability of landfills and cover designs (e.g. Koerner et al. 1986, Negussey et al.

1989, Mitchell et al. 1990, O'Rourke et al. 1990, Takasumi et al. 1991) based on the interface shear strength and design approaches. Landfills are commonly designed to maximize the storage capacity. In some cases the side slopes and cover slopes are designed to be as steep as possible, which pushes the design limits by increasing waste mass and height. These design philosophies sometimes overlook possible effects of progressive failure, shear displacement caused by earthquakes, and continuous changes in the filling geometry and safety during service stages. Hence, a simplified landfill design approach is needed to avoid sudden failures during filling works, induced by unstable filling geometry and seismic effects.

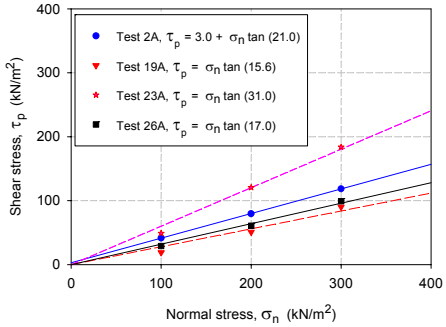

Figure 7 : Interface shear stress results

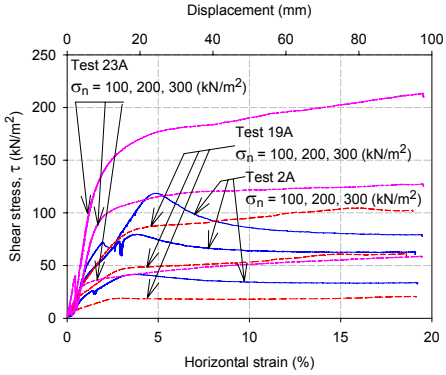

Figure 8 : Stress strain behaviour for the bottom liner shown in Figure 6a.

In order to derive a simplified design approach, the influence of slope sections, normal loads, and seismic loading on liner interface were investigated for factor of safety variation. Four cross sections were adopted for this analysis, namely:

a Case 1 – Landfill of 10m high (H) and 30m width (W), with side slopes of 1V:1H, 1V:2H, 1V:3H, classified as marginally safe under static condition. W/H = 3. As shown in Figure 12a.

b Case 2 – Landfill of 10m high (H) and 50m width (W), with side slopes of 1V:1H, 1V:2H, 1V:3H, classified as moderately safe under static condition. W/H = 5. As shown in Figure 12b.

c Case 3 – Landfill of 10m high (H) and 100m width (W), with side slopes of 1V:1H, 1V:2H, 1V:3H, classified as very safe under static condition. W/H = 10. As shown in Figure 12c.

d Case 4 – Landfill cover with slope of 1V:1H, 1V:2H, 1V:3H, cover soil height of 1m, 2m and 3m (to study the behaviour of cover soil with normal loads) on single lift slope height of 10m. As shown in Figure 12d.

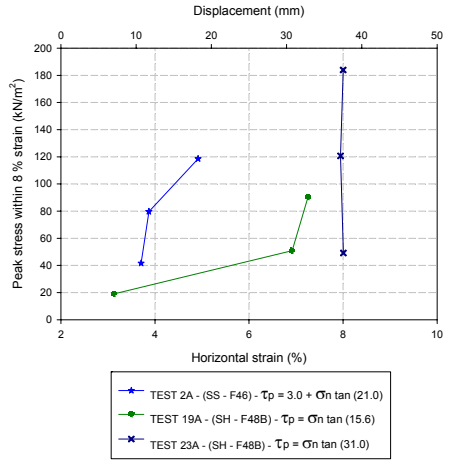

Figure 9 : Peak shear stress with strain plot for the configuration in Figure 6a.

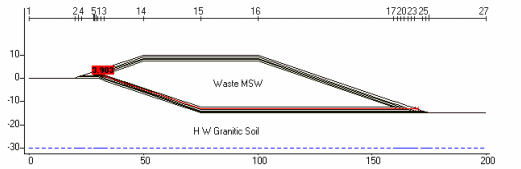

Figure 10 (a) : Typical failure section within the bottom liner in Cases 1 to 5.

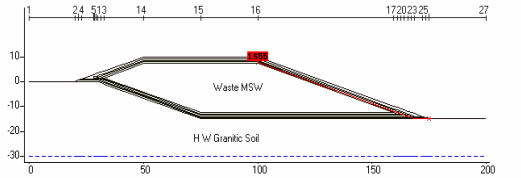

Figure 10 (b) : Typical failure section within the landfill covers in Cases 6 to 9

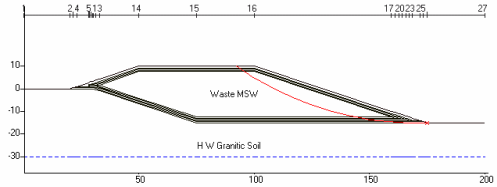

Figure 10 (c) : Toe failure of waste - Case 10

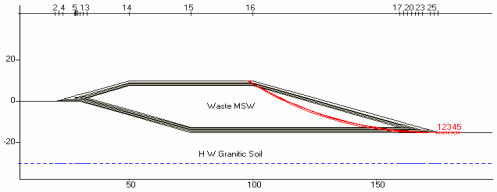

Figure 10 (d) : Overall landfill failure - Case 11

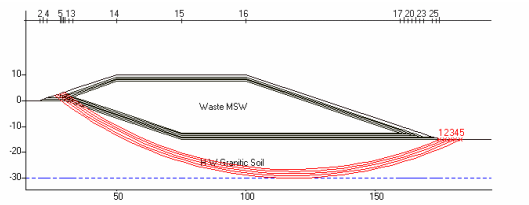

Figure 10 (e) : Overall landfill base failure - Case 12

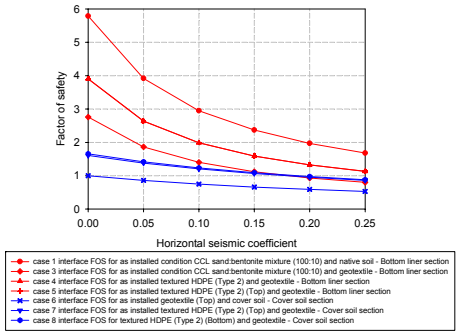

Figure 11a : FOS performance for the interface failure under seismic influence.

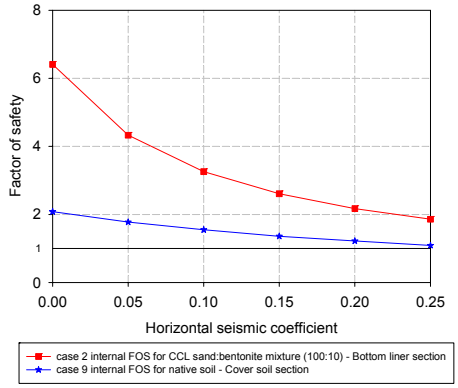

Figure 11b : FOS performance for the internal failure under seismic influence.

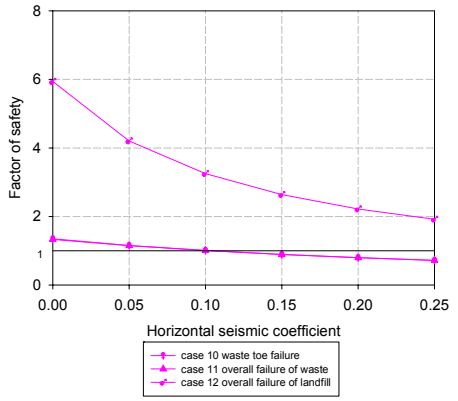

Figure 11c : FOS performance for the overall stability under seismic influence.

In the simplified approach, the adopted assumption is that interface failure is within the interface plane and not cutting through other member components or other interface planes. Hence, the analysis failures were two part wedge and three part wedge mode for the cover slopes and bottom liners, respectively. Table 6 lists the cases analyzed. Cases were individually analyzed for all 49 interface combinations listed in Table 1a, 1b.

The results of the computed FOSs are grouped into two categories namely:

1) Interface stability analysis for the three model landfill liner Cases 1, 2 and 3 (as shown in Figure 12a, 12b and 12c, respectively)
2) Interface stability analysis for the landfill cover slope - Case 4 (as shown in Figure 12d).

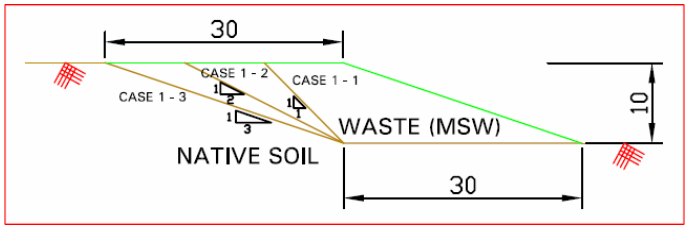

Figure 12a : Case 1 – Landfill of 10m high (H) and 30m width (W), W/H = 3

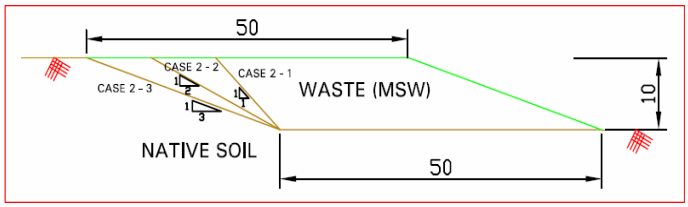

Figure 12b : Case 2 - Landfill of 10m high (H) and 50m width (W), W/H = 5

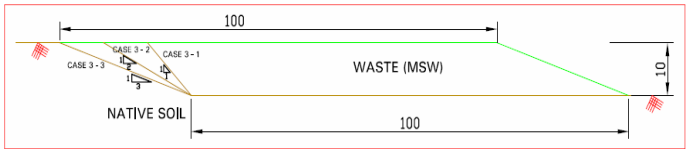

Figure 12c : Case 3 - Landfill of 10m high (H) and 100m width (W), W/H = 10

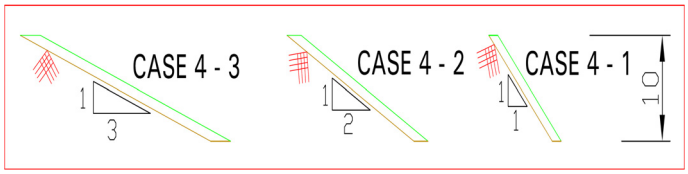

Figure 12d : Case 4 - Landfill cover with slope of 1V:1H, 1V:2H, 1V:3H on a single lift slope height of 10m.

4.1 Base liner stability, Cases 1, 2 and 3

Figures 13a and 13b compile the interface stability for cohesional and frictional resistance, respectively, for Cases 1, 2 and 3. Stability analyses were conducted for all the interface parameters tabulated in Table 1a, 1b. Figures 13a and 13b show that the FOS drops drastically with the seismic coefficient. To have a clearer understanding of the interface performance on the landfill height over width (H/W) factor, trial case with interface cohesion of 20 kN/m^2 and a friction

of 20^0 was computed for FOS and independently plotted for cohesional and frictional against the seismic coefficient.

In Figure 14a, only the cohesional contributions of the FOS for Cases 1, 2 and 3 are plotted. This plot implies that the FOS is sufficient (more than 1.5) under static conditions and as predicted, W/H = 10 has the highest FOS, followed by W/H = 5 and W/H = 3. However, under seismic conditions, the FOS drops drastically with thin marginal differences to no differences between slope factor of W/H = 10, W/H = 5, and W/H = 3 beyond seismic coefficient of 0.1. Only the cohesional contribution from interface is insufficient to withstand seismic loading, which will cause a sudden and drastic collapse of the slope without warning. This is due to the sudden decrease in the FOS crossing unity with seismic loading. In the case of interface frictional contribution as shown in Figure 14b the FOS too reduce drastically with seismic coefficient. Based on Figure 14b, it is observed that FOS drops drastically for W/H = 10 as compared to W/H = 5 or W/H = 3. As the seismic coefficient increases, the drop in the FOS consistently decreases. By combining both cohesion and frictional resistance in Figure 14c, a similar drastic drop in the FOS is also observed. The FOS gradually converges as seismic coefficient increases, indicating that even a very stable slope under static conditions is not necessarily stable under seismic coefficient. However, the FOS is above unity with both the cohesional and frictional resistance contributions. The variation of the back slope angle shows clear differences in FOS under static conditions, however under the influences of seismic forces, the differences in FOS are insignificant. The influence of back slope is also critical, however compared to seismic induced failure, it is not seriously critical. As for the back slope influence on liner geometry, it is found that the FOS is critical for slope angle of 1V:2H relative to angles of 1V:1H and 1V:3H for all cases as shown in Table 7. This is due to the geometry of fill, which provides passive resistance required. As the W/H factor increases, the active forces from 1V:1H back slope is dwarfed due to the large increment in passive resistance against active force provided by 1V:1H back slope. The criticality of the back slope is mitigated from 1V:1H for a low W/H factor to 1V:3H for a higher W/H factor. This trend is closely related solely to the cohesional contribution of the interface FOS as shown in Table 7.

However, for the frictional contribution of interface FOS, the criticality of the geometry is mitigated from 1V:1H to 1V:2H, followed by 1V:3H for W/H of 3, which progressively changes to 1V:2H followed by 1V:3H and 1V:1H for W/H of 5, and finally the 1V:3H seems to be critical for W/H of 10 geometry factor. Hence, engineers can design steep side slopes for landfill liner interface stability, however the filling work should be conducted in a well organized manner to provide sufficient counterbalance, especially against earthquake induced failure.

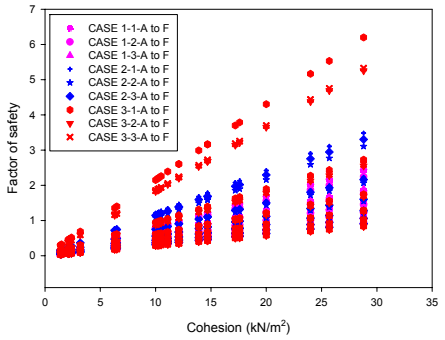

Figure 13a : Plot of cohesional resistance against FOS for Cases 1, 2 and 3 of the base liner.

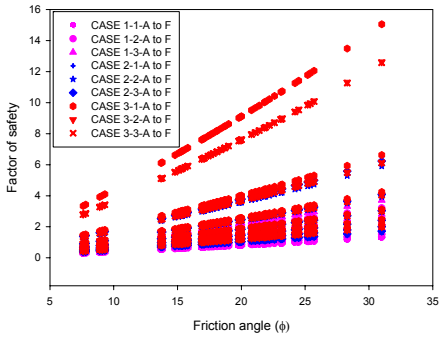

Figure 13b : Plot of frictional resistance against FOS for Cases 1, 2 and 3 of the base liner.

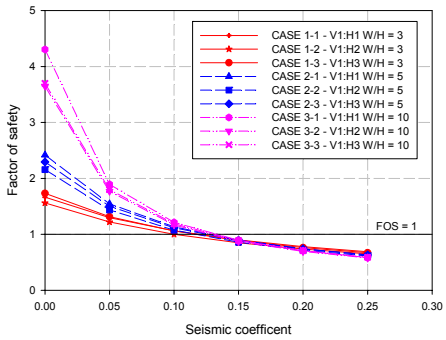

Figure 14a : Plot of FOS with cohesional resistance of 20 kN/m^2 for Cases 1, 2 and 3 of base liner.

4.2 Cover slope liner stability, Case 4

Similar to landfill base liner assessment, the cover slope liner stability assessment was also made on

the interface performance under Case 4, which had slope angles of 1V:1H, 1V:2H and 1V:3H with cover heights of 1m, 2m and 3m. Similar individual assessments were also conducted using only the cohesional and frictional contribution as shown in Figure 14d and 14e, respectively. As for cohesional contribution the FOS increases as the cover slope angle is made gentler from 1V:1H to 1V:3H. However, with increment in cover filling from 1m to 3m the FOS drops accordingly. As for frictional contribution there are no changes in FOS based on cover height increment. The drop in the FOS is solely based on the slope angle. For both frictional and cohesional contributions of cover slope liner stability for the interface in Case 4, the seismic coefficients have no significant effect as compared to Cases 1, 2 and 3.

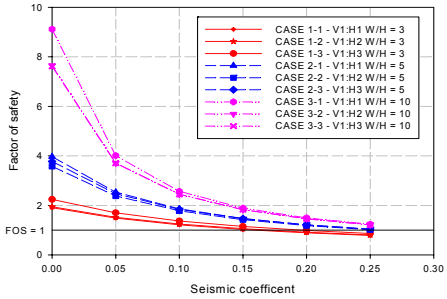

Figure 14b : Plot of FOS with frictional resistance of 20^0 for Cases 1, 2 and 3 of base liner.

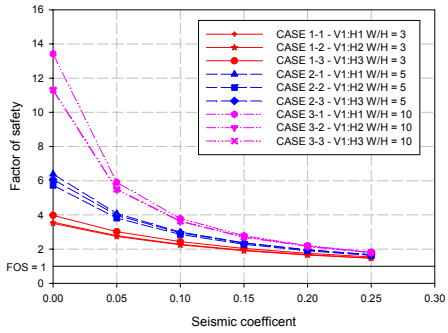

Figure 14c : Plot of FOS with cohesional (20 kN/m^2) and frictional (20^0) resistance for Cases 1, 2 and 3 of base liner.

As for the cover soil fill height and slope angle, it is recommended to have as minimal cover fill as possible not exceeding 0.5m to 1m and as gentle as possible cover slope angle. For the cover soil interface, it is recommended to introduce an interfacing liner with higher cohesional contribution compared to frictional resistance. Figure 14f shows the complied FOS with both cohesion and friction. This is however contrasting with case of Cases 1, 2 and 3 where the frictional resistance of liner interface is critical to provide sufficient stability under seismic loading. Hence, engineers should pay attention on liner material selections and the interface resistance before designing either the base liner or cover slope liner.

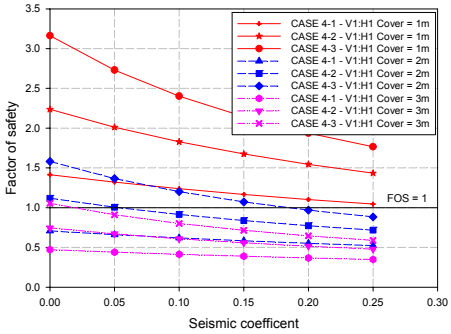

Figure 14d : Plot of FOS with cohesional resistance of 20 kN/m^2 for Case 4 of cover slope.

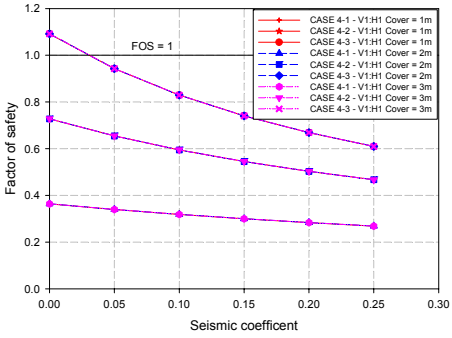

Figure 14e : Plot of FOS with frictional resistance of 20^0 for Case 4 of cover slope

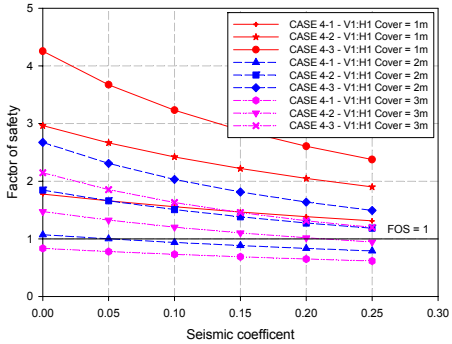

Figure 14f : Plot of FOS with cohesional (20 kN/m^2) and frictional (20^0) resistances for Case 4 of cover slope.

4.3 Landfill liner and cover interface stability prediction

To further simplify the interface stability evaluation, data was complied to produce a computational model and graph to assist engineers to predict the interface FOS of a landfill liner and landfill cover during the design stages and also during the service stages.

The FOS is computed by dividing resisting forces against passive forces such as the shear strength of a failure plane and other stabilizing forces acting on the wedge. Active forces consist of down-slope component weight of the sliding block, forces such as those generated by

seismic acceleration or by water pressures acting on faces of the block, and external forces on the upper slope surface. By using the Mohr Coulomb criteria

$$\tau = c + \sigma_n \tan\phi \qquad (1)$$

$$F = \frac{cL + W\cos\alpha\tan\phi}{W\sin\alpha} \qquad (2)$$

The above equation is further simplified by computing fictional and cohesion contributions individually.

Friction Contribution:

$$FOS_F = \frac{\tan\phi}{\tan\alpha} \qquad (3)$$

Cohesion Contribution:

$$FOS_C = \frac{cL}{W\sin\alpha} \qquad (4)$$

As for the frictional contribution from equation 3, progressive failure could occur in slopes in which the driving force exceeds the mobilized strength of the weakest layer, for example when the slope angle exceeds the friction angle of the interface (Mesri et al., 2003). This function is clearly indicated in Figure 14e where the cover fill height have no influence on FOS and only the cover slope angle has a critical influence. In contrast to the frictional resistance, the cohesional contribution completely depends on the cover height and contact area per unit length. Hence, it is important to balance both cohesional and frictional contribution for FOS under the limit equilibrium design. The compressible nature of MSW is not considered in the limit equilibrium method. This could cause minor over estimation in the FOS based on limit equilibrium method. As for the side slopes, the shear resistance of interface along the side slope is low due to the low normal stress, which depends on the side slope angle and interface frictional resistance along the side slope. This results in a shear displacement along the weakest interface in a side slope liner system, which mobilizes the passive resistance of the MSW along the base of the landfill. This stress transfer mechanism is especially relevant to MSW due to the compressible nature of MSW (Stark et al., 2004). This stress transfer phenomenon has been duplicated using numerical methods by Gilbert et al. (1996) and Reddy et al. (1996).

4.4 Seismic influence on landfill base and cover liner factor of safety

Seismic effects are incorporated in the limit equilibrium analysis where the forces induced by earthquake accelerations were treated as horizontal forces. Although vertical forces are also caused by an earthquake, these forces were not computed into the analysis. The horizontal force (F_h), due to an earthquake is assumed to act through the centre of gravity of soil mass involved in predicting the failure as:

$$F_h = kw = k\,mg \qquad (5)$$

Where m is the mass of the soil and k is the seismic coefficient. Thus, the seismic coefficient k is a measurement of the earthquake acceleration in terms of g. Table 8 shows the calculation, while Figure 15 shows the computation model.

FOS from Friction = $FOS_F = \tan\phi * (P/A)$ (6)

FOS from Cohesion = $FOS_C = \tan\phi * (L/A)$ (7)

Total FOS = $FOS_F + FOS_C$ (8)

Where P is the Passive Resistance, A is the Active Forces, and L is the Total Interface Length. In order to understand, predict, and monitor the continuous trend of the FOS during filling and maintenance work, each FOS is computed individually based on the frictional and cohesional contributions. Figures 16a and 16b show the individual plots of the FOS based on the frictional and cohesional contributions, respectively, with the coefficient of active forces and passive resistance incorporated.

The frictional contribution of the FOS tends to have an exponential increment with friction angle. As shown in Figure 16a, the higher the value of passive resistance against active forces (P/A) the higher the FOS. However in Figure 20b the FOS increases linearly with cohesion. The incorporated plot of the Interface Length/Active Forces (L/A) allows the FOS to be estimated based on cohesion parameters. The total predicted FOS can be low as 1.1 or 1.3 as the computed coefficients of P/A and L/A has incorporated all the active and destabilising forces, including seismic loading.

Example of FOS prediction, Say interface parameters with cohesion of 20 kN/m^2 and frictional resistance of 20^0, would be:

$$\tau = 20 + \sigma_n \tan 20^0 \qquad (9)$$

In order to obtain a FOS above unity, a minimum Passive Resistance/Active Forces (P/A)

of 2.9 and Interface Length/Active Forces (L/A) of 0.05 are sufficient. The combined frictional and cohesional resistance contribute to a total FOS of 2.0. Similar prediction plot was also made for a cover slope for P/A and L/A in Figure 18a and 18b respectively. Table 9 shows the sample calculation for the cover liner interface computation model shown in Figure 17. The toe passive resistance was ignored in the computation. In the case of the cover slope, the friction contribution has a minor contribution to the total FOS. The data in Figure 16a and 18a are combined in Figure 19a and used to predict the FOS over a wide range of P/A (Passive Resistance/Active Forces). Similarly, the data in Figure 16b and 18b are combined in Figure 19b and used to predict the FOS over a wider range of L/A (Interface Length/ Active Forces).

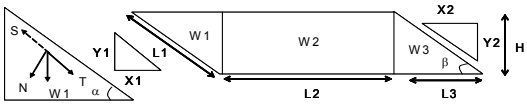

Figure 15 : Landfill base liner interface stability computation model.

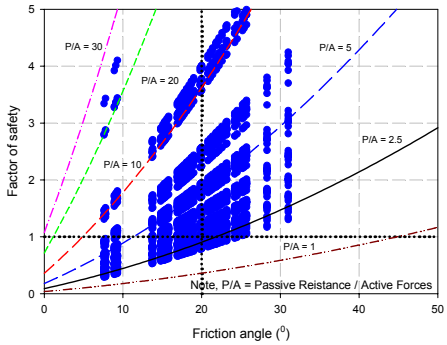

Figure 16a : Prediction of interface FOS based on P/A (Passive Resistance/Active Forces) for base liner stability for frictional resistances.

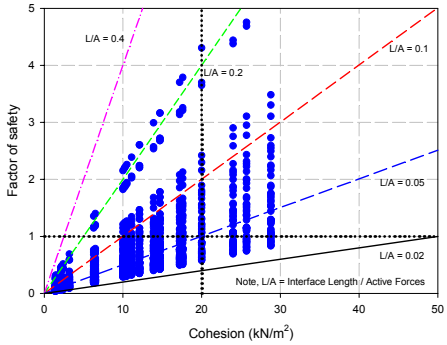

Figure 16b : Prediction of interface FOS based on L/A (Interface Length/Active Forces) for base liner stability for cohesional resistance.

5 CONCLUSION

As for liner design, it is recommended to configure the liner members to act as a composite member during failure. The composite behaviour could cause the failing interface plane to cut through other interface planes and indirectly gain resisting strength during failure. Hence, understanding the stress and horizontal strain behaviour of liner member components is critical in order to allow the transfer of failure stress between interfacing members to resist continuous or progressive failure from occurring. The proposed method to analyze the interface stress and horizontal strain behaviour in order to understand the failure trend could assist design engineers in evaluating the performance of an individual interfacing member, which may identify the possibility of a composite or non-composite failure mode based on fill height (normal stresses). This evaluation would improve the selection of liner members, the orientation or placement methodology, and the material properties.

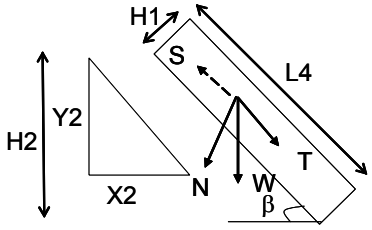

Figure 17 : Landfill cover liner interface stability computation model.

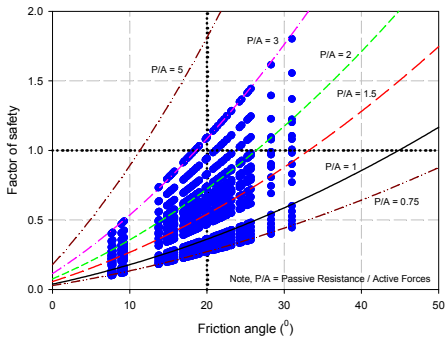

Figure 18a : Prediction of interface FOS based on P/A (Passive Resistance/Active Forces) for cover slope stability for frictional resistance.

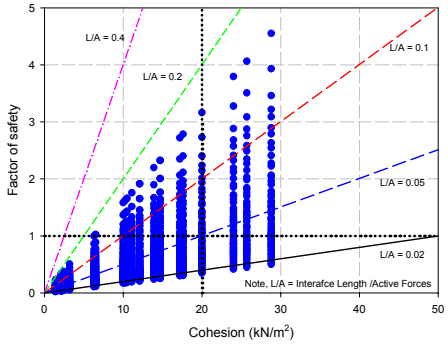

Figure 18b : Prediction of interface FOS based on L/A (Interface Length/Active Forces) for cover slope stability for cohesional resistance.

As for frictional and cohesional contributions of the interface parameters, it is recommended to introduce an interfacing liner with a higher cohesional contribution compared to frictional resistance for cover soil liners due to the low normal loads (shallow fill height). However, for bottom liners, frictional resistance had significant influence on interface stability due to high normal loads and counter balancing geometry. Along with stability and interface property assessment engineers are required to carefully select the liner configuration with a suitable stress and horizontal strain behaviour at the preliminary peak stages and at the post peak stresses in the residual region in order to design a well-integrated composite design.

The FOS assessment depends on the landfill geometry, liner interface properties, and external disturbing forces such as seismic loading. Hence, engineers are required to balance the active and passive resistance forces (P/A), and the interface length with active forces (L/A) to prevent a sudden and drastic drop in the FOS during an earthquake. Hence, it is vital to continuously assess the FOS or to monitor the FOS while filling to ensure the landfill site is stable at all times in order to resist external destabilizing forces. This finding also indicates that not all safe slopes are actually stable under seismic conditions, when it comes to an interface induced failure. Hence, the proposed FOS prediction method could be a useful guide for engineers. The advantage of the proposed FOS prediction methods are:

- Will be quick reference for engineers when selecting liner materials based on interface test properties.
- Can obtain initial estimation of the FOS based on site geometry or back slope conditions.
- Useful for designing the appropriate anchorage methods for liners to obtain an adequate FOS.
- Useful to perform continuous monitoring of the FOS at a landfill site while filling work is in progress.
- Assist in organizing a sequential filling to maintain an adequate FOS for both static and seismic conditions.
- If the FOS is found to be inadequate appropriate steps can be taken immediately to avoid sudden failures by reorganising the filling lift to provide sufficient counter balance.
- Useful for site engineers to safely coordinate ongoing filling work.

6 REFERENCES

Chiu, P. and Fox, P.J. (2004). Internal and interface shear strengths of unreinforced and needle-punched geosynthetic clay liners, *Geosynthetics International,* 11, No.3, 176–199.

Daniel, D.E. Koerner, R.M., Bonaparte, R., Landreth, R.E., Carson, D.A., and Scranton, H.B. (1998). Slope stability of geosynthetic clay liner test plots, *Journal of Geotechnical and Geoenvironmental Engineering,* ASCE, 124, No.7, 628-637.

Dove, J. E. and Frost, J. D. (1999). Peak friction behavior of smooth geomembrane-particle interfaces, *Journal of Geotechnical and Geoenvironmental Engineering*, ASCE, 125, No. 7, 544-555.

Eid, H. T., Stark, T. D., Evans, W. D. and Sherry, P. (2000). Municipal solid waste landfill slope failure I: foundation and waste properties. *Journal of Geotechnical and Geoenvironmental Engineering*, ASCE, 126, No. 5, 397-407.

Filz, G. M., Esterhuizen, J. J. B. and Duncan, J. M. (2001). Progressive failure of liner waste impoundments. *Journal of Geotechnical and Geoenvironmental Engineering*, ASCE, 127, No. 10, 841-848.

Fox, P. J., Rowland, M. G. and Scheithe, J. R. (1998). Internal shear strength of three geosynthetic clay liners. *Journal of Geotechnical and Geoenvironmental Engineering*, ASCE, 124, No. 10, 933-944.

Fox, P. J. and Stark, T. D. (2004). State-of-the-art report: GCL shear strength and its measurement, *Geosynthetics International,* 11, No.3, 141–175.

Gilbert, R. B. and Byrne, R. J. (1996). Strain-softening behavior of waste containment system interfaces. *Geosynthetics International*, 3. No. 2, 181-203.

Gourc, J.P. and Reyes Ramirez, R. (2004). Dynamics-based interpretation of the interface friction test at the inclined plane, *Geosynthetics International,* 11, No.6, 439–454.

Hoe I. Ling and Dov Leshchinsky, (1997). Seismic stability and permanent displacement of landfill cover systems, *Journal of Geotechnical and Geoenvironmental Engineering*, pp. 113-112.

Koerner, R. M., Martin, J. P. and Koerner, G. R. (1986). Shear Strength parameters between geomembranes and cohesive soils. *Geotextiles and a*

Kotake, N., Watanabe, K., Nonomura, C., and Negishi, K. (2004): Interactive behaviors of

geosynthetics multi-layer systems under shear force, *GeoAsia2004, Proceedings of the 3rd Asian Regional Conference on Geosynthetics,* J.B. Shim, C. Yoo, and H.-Y. Jeon (eds.), 937-944.

Ling, H.I. and Leshchinsky, D. (1997). Seismic stability and permanent displacement of landfill cover systems, *Journal of Geotechnical and Geoenvironmental Engineering,* ASCE, 123, No.2, 113-122.

Long, J. H., Gilbert, R. B. and Daly, J. J. (1995). Effect of waste settlement on sloped lining systems. *Proceeding of Geosynthetics* '95, Nashville, TN, 2, 729-744.

McKelvey, J. A. III (1994). Consideration of equipment loadings in geosynthetic lined slope designs. *Proceedings of the 8th International Conference on Computer Methods and Advances in Geomechanics*, Rotterdam, 2, 1371-1377.

Mesri, G. and Shahien, M. (2003). Residual shear strength mobilized in first-time slope failures: *Journal of Geotechnical and Geoenvironmental Engineering*, ASCE, 129, No. 1, 12-31.

Mitchell, J. K., Seed, R. B. and Seed, H. B. (1990). Kettleman Hills waste landfill slope failure I: liner-system properties. *Journal of Geotechnical Engineering*, ASCE, 116, No. 4, 647-668.

Negussey, D., Wijewickreme, W. K. D. and Vaid, Y. P. (1989). Geomembrane interface friction. *Canadian Geotechnical Journal*, 26, No. 1, 165-169.

O'Rourke, T. D., Druschel, S. J. and Netravali, A. N. (1990). Shear strength characteristics of sand polymer interfaces. *Journal of Geotechnical Engineering*, ASCE, 116, No. 3, 451-469.

Palmeira, E.M., Lima, N. R. Jr, and Mello, L.G.R. (2002). Interaction between soils and geosynthetic layers in large-scale ramp tests, *Geosynthetics International,* .9, No.2, 149–187

Reddy, K. R., Kosgi, S. & Motan, S. (1996). Interface shear behavior of landfill composite liner systems: a finite element analysis. *Geosynthetics International,* 3, No. 2, 247-275.

Saravanan M., Kamon M., Faisal H. A., Katsumi T., Akai T., Inui T., Matsumoto A. (2006a). Landfill Stability Assessment Using Interface Parameters, *Proceeding of the 6th Japan-Korea-France Joint Seminar on Geoenvironmental Engineering*, 2006, Japan. 137-146

Saravanan M., Kamon M., Faisal H. A., Katsumi T., Akai T., Inui T., Matsumoto A. (2006b). Interface Shear Stress Parameter Evaluation for Landfill Liner using Modified Large Scale Shear Box, *Proceedings of the 8th International Conference on Geosynthetics, 2006, Conference, Japan*. J. Kuwano and J. Koseki (eds). 265-271

Saravanan M., Kamon M., Faisal H. A., Katsumi T., Akai T., Inui T., Matsumoto A. (2006c). Interface performances of geotextiles, geomembranes, GCLs and CCLs for landfill liner stability. *Geotextitle and Geomembrane* (under review)

Stark, T. D. and Choi H. (2004). Peak versus residual interface strengths for landfill liner and cover design. *Geosynthetics International*, 11, No. 6, 491-498

Stark, T. D. and Poeppel, A. R. (1994). Landfill liner interface strengths from torsional ring shear tests. *Journal of Geotechnical Engineering*, ASCE, 120, No. 3, 597-615.

Stark, T. D., Williamson, T. A. and Eid, H. T. (1996). HDPE geomembrane/geotextile interface shear strength. *Journal of Geotechnical Engineering*, ASCE, 122, No.3, 197-203.

Stark, T. D. Eid, H. T., Evans, W. D. and Sherry, P. (2000). Municipal solid waste landfill slope failure II: stability analyses. *Journal of Geotechnical and Geoenvironmental Engineering*, ASCE, 126, No. 5, 408-419.

Takasumi, D. L., Green, K. R. and Holtz, R. D. (1991). Soil-geosynthetic interface strength characteristics: a review of state-of-the-art testing procedures. *Proceedings of Geosynthetics '91 Conference,* Atlanta, GA, 1, 87-100.

Yazdani, R., Campbell, J. L. and Koerner, G. R. (1995). Long-term in situ measurements of a high density polyethylene geomembrane in a municipal solid waste landfill. *Proceedings of Geosynthetics* '95, Nashville, TN, 3, 893-905.

7 NOTATION

L = Length of failure plane
τ = Total shear strength
c = Total cohesion
W = Total weight acting on the failure plane
α = Side slope angle
β = Cover slope angle
ϕ = Total friction angle
σ_n = Total normal stress on failure plane
F = Factor of safety
P1, P2, P3 = Passive forces on individual landfill blocks

Table 1a : Various combinations of the laboratory interface tests.

Interfacing material	Geotextile	Smooth HDPE (Type 1)	Textured HDPE (Type 2)	Rear side of PVC	Front side of PVC	Bentonite side of bentonite -glued GCL (Type 1)	HDPE side of bentonite -glued GCL (Type 1)	Non woven side of needle-punched GCL (Type 2)	Woven side of needle-punched GCL (Type 2)	Native soil
Smooth HDPE (Type 1)	Test 1A									
Textured HDPE (Type 2)	Test 2A									
Rear side of PVC	Test 3A									
Front side of PVC	Test 3C									
Bentonite side of bentonite-glued GCL (Type 1)	Test 4A	Test 6A	Test 8A	Test 10A	Test 10E					
HDPE side of bentonite-glued GCL (Type 1)	Test 4C	Test 6C	Test 8C	Test 10C	Test 10G					
Non woven side of needle-punched GCL (Type 2)	Test 5A	Test 7A	Test 9A	Test 11A	Test 11E					
Woven side of needle-punched GCL (Type 2)	Test 5C	Test 7C	Test 9C	Test 11C	Test 11G					
Silt:bentonite mixture (100 : 10)	Test 12A	Test 13A	Test 14A	Test 15A	Test 15C	Test 17A	Test 17C	Test 18A	Test 18C	Test 16A
Sand:bentonite mixture (100 : 10)	Test 19A	Test 20A	Test 21A	Test 22A	Test 22C	Test 24A	Test 24C	Test 25A	Test 25C	Test 23A
Native soil	Test 26A	Test 27A	Test 28A	Test 29A	Test 29C					

P = Total passive force
A1, A2, A3 = Active forces on individual landfill blocks
A = Total active force
N = Normal load
F_h = Horizontal force
m = Mass of waste
k = Seismic coefficient
g = Gravity acceleration
H = Fill height
H1 = Cover fill height
H2 = Cover slope height
W1, W2, W3 = Landfill block total weight
X1, X2 = Horizontal distance
Y1, Y2 = Vertical distance
L1, L2, L3 = Length of interface failure plane in a landfill block
L4 = Cover liner interface length
S = (W1) * cos (α or β)
T = (W1) * sin (α or β)

Table 3 : Liner configurations and interface tests for single membrane liner configuration 1 (SMLC 1).

Liner configuration	Interface test	Description	Interface parameter		Stress and horizontal strain
			Cohesion (kN/m²)	Friction angle (°)	
SMLC A	Test 1A	Geotextile and smooth HDPE (Type 1)	0.0	7.6	SH - F13
	Test 27A	Smooth HDPE (Type 1) and native soil	0.0	15.6	SH - F13
SMLC B	Test 2A	Geotextile and textured HDPE (Type 2)	3.0	21.0	SS – F35
	Test 28A	Textured HDPE (Type 2) and native soil	0.0	23.0	SH – F48B
SMLC C	Test 3C	Geotextile and fronts side of PVC	26.3	16.9	SC – F48B
	Test 29A	Rear side of PVC and native soil	0.0	18.7	SC – F35

Table 4 : List of soil parameters and interface test results.

Test	Description	Cohesion (kN/m²)	Friction Angle (°)	Bulk Density (Mg /m³)
Interface Parameters				
Test 2A	Interface between geotextile and geomembrane textured HDPE (Type 2) - as installed condition	3.0	21.0	-
Test 19A	Interface between compacted clay liner – sand:bentonite mixture (100:10) and geotextile – as installed condition	0.0	15.6	-
Test 23A	Interface between compacted clay liner – sand:bentonite mixture (100:10) and native soil – as installed condition	0.0	31.0	-
Test 26A	Interface between geotextile and native soil – as installed condition	0.0	17.8	-
Soil Parameters				
1	Highly weathered granite soil (native soil)	0.0	35.0	2.4
2	Compacted clay liner – Sand:bentonite mixture (100:10)	0.0	33.5	1.9
3	Waste (MSW) - Qian X, 2002	10.0	18.0	1.5

Table 5: Stability cases considered for analysis.

Case	Description
Case 1	Interface falure between compacted clay liner – Sand:bentonite mixture (100:10) and native soil
Case 2	Internal failure of compacted clay liner – Sand:bentonite mixture (100:10)
Case 3	Interface failure between compacted clay liner – Sand:bentonite mixture (100:10) and geotextile
Case 4	Interface between geotextile and geomembrane Textured HDPE (Type 2) – Bottom
Case 5	Interface between geotextile and geomembrane Textured HDPE (Type 2) – Top
Case 6	Interface between geotextile and cover soil (highly weathered granitic soil – native soil)– Top
Case 7	Interface between geotextile and geomembrane Textured HDPE (Type 2) – Top
Case 8	Interface between geotextile and geomembrane Textured HDPE (Type 2) – Bottom
Case 9	Internal failure of cover soil (highly weathered granitic soil – native soil)
Case 10	Toe failure of waste
Case 11	Overall landfill failure
Case 12	Overall landfill base failure

Table 1b : Various combinations of the laboratory interface test results.

Interfacing material c: cohesion in kN/m^2 ϕ: frictional angle in degree.	Geotextile		Smooth HDPE (Type 1)		Textured HDPE (Type 2)		Rear side of PVC		Front side of PVC		Bentonite side of bentonite -glued GCL (Type 1)		HDPE side of bentonite -glued GCL (Type 1)		Non woven side of needle-punched GCL (Type 2)		Woven side of needle-punched GCL (Type 2)		Native soil	
	c	ϕ	c	ϕ	c	ϕ	c	ϕ	c	ϕ	c	ϕ	c	ϕ	c	ϕ	c	ϕ	c	ϕ
Smooth HDPE (Type 1)	0.0	7.6																		
Textured HDPE (Type 2)	3.0	21.0																		
Rear side of PVC	11.3	18.6																		
Front side of PVC	26.3	16.9																		
Bentonite side of bentonite-glued GCL (Type 1)	11.5	17.2	0.0	9.0	28.9	18.7	19.0	17.7	0.0	24.5										
HDPE side of bentonite-glued GCL (Type 1)	0.0	21.8	2.2	8.9	0.0	19.8	11.8	20.0	0.0	25.1										
Non woven side of needle-punched GCL (Type 2)	1.3	15.0	2.3	7.7	10.4	25.4	17.0	15.2	11.0	17.0										
Woven side of needle-punched GCL (Type 2)	10.6	14.7	2.4	9.2	2.5	22.9	14.4	18.0	22.8	18.4										
Silt:bentonite mixture (100 : 10)	0.0	15.2	0.0	15.3	0.0	24.1	0.0	22.2	0.0	19.8	13.9	16.9	0.0	22.5	6.1	20.8	1.7	21.2	10.3	28.3
Sand:bentonite mixture (100 : 10)	0.0	15.6	0.0	13.7	0.0	24.5	0.0	19.7	0.0	16.9	6.7	17.4	15.3	13.5	0.0	22.6	0.0	22.4	0.0	31.0
Native soil	0.0	17.8	0.0	15.6	0.0	23.0	0.0	18.7	0.0	20.2										

Table 2 : Interface stress strain behaviour of the interface test results.

Interfacing material	Geotextile	Smooth HDPE (Type 1)	Textured HDPE (Type 2)	Rear side of PVC	Front side of PVC	Bentonite side of bentonite -glued GCL (Type 1)	HDPE side of bentonite -glued GCL (Type 1)	Non woven side of needle-punched GCL (Type 2)	Woven side of needle-punched GCL (Type 2)	Native soil
Smooth HDPE (Type 1)	SH – F13 0.7-0.9*									
Textured HDPE (Type 2)	SS – F35 3.7-4.9*									
Rear side of PVC	SH – F48B 5.1-8.0B*									
Front side of PVC	SC – F48B 5.6-8.0B*									
Bentonite side of bentonite-glued GCL (Type 1)	SS – F35 4.1-4.8*	SH - F13 1.1-1.8*	SC - F35 3.0-3.8*	SH – F48B 5.6-8.0B*	SH - F13 1.6-8.0B*					
HDPE side of bentonite-glued GCL (Type 1)	SS – F35 4.2-4.5*	SH – F48B 7.8-8.0B*	SH – F35 3.4-4.1*	SH - F13 1.0-1.4*	SH - F13 1.7-2.0*					
Non woven side of needle-punched GCL (Type 2)	SS – F35 3.1-4.0*	SH - F13 1.1-1.6*	SS – F35 3.1-4.5*	SH - F46 4.6-6.1*	SH – F48 4.4-7.8*					
Woven side of needle-punched GCL (Type 2)	SH – F35 3.9-4.4*	SH - F13 0.9-1.6*	SS – F35 2.7-4.1*	SC - F48 5.1-8.0*	SC – F48B 4.2-8.0B*					
Silt:bentonite mixture (100:10)	SH – F46 4.5-5.7*	SH - F13 1.2-1.9*	SC – F48B 5.0-8.0B*	SC – F48 3.3-7.9*	SC – F48 3.4-7.8*	SH - F46 4.4-6.0*	SC – F48B 5.7-8.0B*	SC – F48 5.8-7.2*	SC – F48 5.5-7.8*	SH – F48B 7.8-8.0B*
Sand:bentonite mixture (100:10)	SH – F48 3.1-7.3*	SH - F13 0.8-1.9*	SH – F48B 8.0B*	SC – F48B 5.8-8.0B*	SC – F48B 3.8-8.0B*	SH – F13 2.5-3.6*	SC – F48B 5.6-8.0B*	SC – F48B 4.0-8.0B*	SC – F48B 6.7-8.0B*	SH – F48B 8.0B*
Native soil	SC – F48 4.2-7.9*	SH - F13 1.1-2.8*	SH – F48B 7.0-8.0B*	SC - F35 2.8-4.7*	SC - F35 1.7-3.0*					

SH: Horizontal strain hardening behavior for all normal stress levels tested.
SS: Horizontal strain softening behavior for all normal stress levels tested.
SC: Stress and horizontal strain behavior depends upon the normal stress levels. Horizontal strain hardening for low normal stress and softening for high normal stress.
F13, F35, or F46: Failure occurred within the 1-3%, 3-5%, or 4-6% of horizontal strain respectively.
F48B: Failure occurred within the 4-8% horizontal strain or beyond.
* - Horizontal strain at peak shear stress

Table 6 : List of cases analyzed.

Case	Width / Height (W/H)	Back slope angle	Seismic coefficient
1	3	1H : 1V	0.05
			0.10
		2H : 1V	0.15
			0.20
		3H : 1V	0.25
2	5	1H : 1V	0.05
			0.10
		2H : 1V	0.15
			0.20
		3H : 1V	0.25
3	10	1H : 1V	0.05
			0.10
		2H : 1V	0.15
			0.20
		3H : 1V	0.25
Case	**Cover slope angle**	**Cover fill height (m)**	**Seismic coefficient**
4a	1H : 1V	1	0.05
			0.10
		2	0.15
			0.20
		3	0.25
4b	2H : 1V	1	0.05
			0.10
		2	0.15
			0.20
		3	0.25
4c	3H : 1V	1	0.05
			0.10
		2	0.15
			0.20
		3	0.25

Table 7: Summary of FOS under static conditions for cohesion of 20 kN/m^2 and friction of 20^0 for Cases 1, 2 and 3.

Back slope angle	Width / Height of fill geometry (W/H)	Interface Factor of Safety for cohesion of 20 kN/m^2 and friction of 20^0				Total FOS	Combined critical factor
		Cohesion		Friction			
		FOS	Critical factor	FOS	Critical factor		
1V : 1H	W/H = 3	1.67	2	1.91	1	3.58	2
1V : 2H	(Case 1)	1.56	1	1.95	2	3.51	1
1V : 3H		1.73	3	2.24	3	3.97	3
1V : 1H	W/H = 5	2.42	3	3.97	3	6.39	3
1V : 2H	(Case 2)	2.16	1	3.58	1	5.74	1
1V : 3H		2.29	2	3.78	2	6.07	2
1V : 1H	W/H = 10	4.30	3	9.11	3	13.41	3
1V : 2H	(Case 3)	3.65	1	7.65	2	11.30	1
1V : 3H		3.70	2	7.61	1	11.31	2

Table 8: Computations approach for the landfill liner interface stability.

Passive Resistance		**Active Forces**	
(W1)*cos α	= P1 kN/m	(W1)*sin α	= A1 kN/m
W2	= P2 kN/m	Seismic active forces	
W3	= P3 kN/m	W1 * (k)	= A2 kN/m
Total Passive Forces		W2 * (k)	= A3 kN/m
P1 + P2 + P3	**= P kN/m**	W3 * (k)	= A4 kN/m
Total Interface Length		**Total Active Forces**	
L1 + L2 + L3	**= L m**	A1 + A2 + A3 + A4	**= A kN/m**
Friction	Passive Resistance / Active Forces or P/A		
Cohesion	Interface Length /Active Forces or L/A		

Table 9 : Computations approach for cover slope interface stability

Passive Resistance		**Active Forces**	
S = (W)*cos β	= P kN/m	T = (W)*sin β	= A1 kN/m
Total Passive Forces		Seismic active	
	P kN/m	W * (k)	= A2 kN/m
Total Interface Length		**Total Active Forces**	
L4	**= L m**	A1 + A2	**= A kN/m**
Friction	Passive Resistance / Active Forces or P/A		
Cohesion	Interface Length /Active Forces or L/A		